*International Journal of Engineering and Science Invention (IJESI)*
*ISSN (Online): 2319-6734, ISSN (Print): 2319-6726*
*www.ijesi.org ||Volume 14 Issue 4 April 2025 || PP 136-143*

# Modeling and Simulation of Hybrid Electric Vehicles

Vinay Kumar[1] , Gyanendra Yadav [2]
*Scholar M.Tech(M.E) VGI Gr.Noida[1] , Asst. Prof, Dept. of M.E, ) VGI Gr.Noida [2]*

***ABSTRACT***
*A comprehensive multi-physics approach to hybrid electric vehicle (HEV) modeling is presented in this work. Purpose of model is to enable design engineers to create regulator structures & automated optimization procedures for HEVs, as well as to examine the consequences of component selection. Internal combustion engine (ICE), motor producer (MG), power split device (PSD), and longitudinal dynamics of the vehicle are all part of the whole drivetrain organization of a series/parallel HEV.*

*Every facet of friction, damping, stiffness, and rotational inertial dynamics is taken into account. The MATLAB/Simulink/Simscape blockset environment is used to implement the interactions between all of these components. The model creation process places a strong emphasis on the ideas of modularity, adaptability, and an intuitive user interface. The identical hybrid power train's analytical and numerical simulation results are contrasted. The model is useful for upcoming HEV optimization approaches because of the convergence of the findings.*

***KEY WORDS: Hybrid vehicles, MATLAB/SIMULINK, modelling, simulation, PSD.***

## I. INTRODUCTION

The scarcity of petroleum supplies and rising pollution levels have prompted global automotive research to look for cleaner and more sustainable energy sources throughout the last ten years. Both demand and production rates are increasing quickly, despite the fact that finite fossil fuel supplies are steadily being depleted [1-2]. A hybrid electric vehicle (HEV) has been proposed as a temporary fix to lower hazardous emissions and increase fuel efficiency [3]. It is well known that hybrid electric vehicles (HEVs) lessen reliance on petroleum fuels by combining two energy sources: electric propulsion systems and traditional internal combustion engines.

Additionally, the dual power source approach allows for engine downsizing, load balancing, and range extension. Regardless of the vehicle's power requirements, proper engine size allows the engine to run close to its economic conditions, resulting in lower emission levels.

In general, there are three fundamental configurations of HEVs based on the architecture of hybrid propulsion: series, parallel, and series/parallel. In a series HEV, the generator transforms the engine's mechanical energy into electrical energy. As shown in Figure 1-a, this electric energy is stored in the battery pack and then transformed once more into mechanical energy by the electric motors to move the vehicle forward. This type's primary advantages are its ease of installation and operation, but its primary drawbacks include double energy conversion. Additionally, the powertrain redundancy is decreased by the serial power flow.

Additionally, the powertrain redundancy is decreased by the serial power flow. As seen in Figure 1-b, a parallel HEV is powered by a combination of electric motor power and engine mechanical power. Although this arrangement offers more operational options, it is practically challenging to integrate into the drivetrain. The benefits of the previously stated architectures are combined in the series/parallel HEV arrangement, which offers the option of using the electric and mechanical energies concurrently or sequentially. However, as Figure 1-c illustrates, one of its primary disadvantages is the difficulty of assembly.

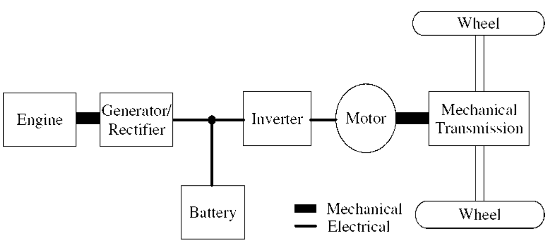


(a) The Architecture of A Series HEV

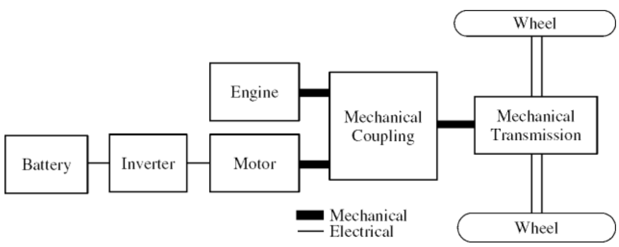


(b) The Architecture of a Parallel HEV

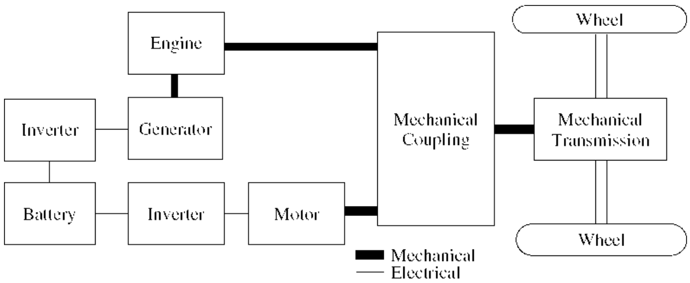


(c) The Architectures of a Series/Parallel HEV
**Fig. 1** Hybrid Vehicle Topologies.

Better comprehension and control of HEV functioning are made possible by accurate modeling and simulation. Khan created a model for "Honda Integrated Motor Assist" (IMA) in the MATLAB/Simulink environment, which is one of the well-known published works. During two distinct conventional driving cycles, three parameters—fuel consumption, regenerated energy, and consumed energy—were taken into account and contrasted. An optimization approach for the series/parallel "Toyota Hybrid System" (THS) was presented by Peng and Liu [1,6]. Subsequently, they examined the debate between rule-based optimization and bettering the powertrain design or component size for the "Toyota Hybrid System" (THSII). Another control technique was created by Peng et al. for the parallel HEV model that takes into account an adaptive energy management control system. A MATLAB/Simulink model was presented by Stein et al. to implement a dynamic programming approach. Wipke et al. created a simulator to model the entire HEV powertrain using ADVISOR. methods. Because of its widespread use in contemporary automobiles, special attention is given to the modeling of series and parallel HEVs.

Although the examined work has advanced the state of the art in HEV, it should be highlighted that the majority of them were either restricted to limited access simulators or specialized to a particular hybrid topology. Nonetheless, more general models that are still sufficient to adequately depict HEV performance must be created. This article presents a simplified model with code that may be used to alter its subsystems and exposed to additional optimization

## THE MODEL DISCRIPTION

The major component of the series/parallel HEV is a power split mechanism that combines power from the engine and an electric motor generator (MG). Figure 2 shows how the PSD's output power is delivered to the wheels via the propeller shaft, open differential, and rear axle.

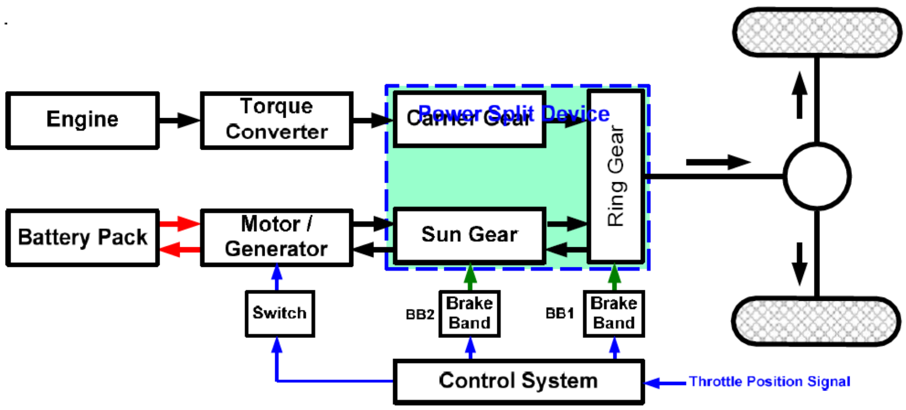


**Fig. 2** The Main Layout of the HEV Model.

The Simscape blockset library, which includes the Sim Driveline, Sim Electronics, and Sim Control Schemes tool boxes, is used to model and implement these components [17]. The Simscape blockset is a component of Simulink corporeal modeling, which includes designing and modeling systems based on fundamental physical concepts. Physical modeling operates inside the Simulink environment and integrates easily with MATLAB and the rest of Simulink. A HEV drivetrain system may be represented with a linked block illustration thanks to physical modeling blocks, which directly represent physical components or relationships, in contrast to other Simulink blocks that reflect mathematical processes.

As shown in Figure 3, the model incorporates the engine characteristics as a look-up table of machine torque vs engine speed and throttle position. In a driveline, actuators can start and sustain rotation while sensors measure the driveline parts' movements and the torques applied to them. The physical properties depicted in Figure 4 are used to model the torque converter.

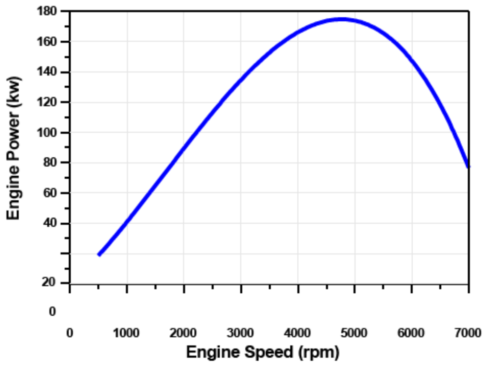


**Fig. 3.** Engine Characteristics.

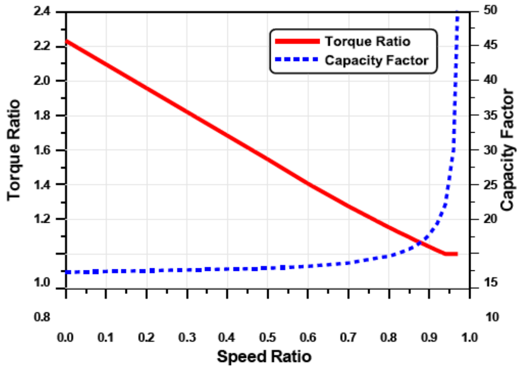


**Fig. 4**. Torque Converter Characteristics.

The armature resistance, or R, is a representation of the equivalent circuit of a DC motor. The inductance L is believed to have no influence on the steady-state torque-speed relationship. Taking into account the damping (J) and motor inertia (J), The torque that the DC motor produces, T, is proportional to the armature current, magnetic field intensity, and rotational speed.

$$T = k_t \cdot \underbrace{\left( \frac{V - k_v \cdot \omega}{R} \right)}_{Armature\ Current} - J \cdot \dot{\omega} - \gamma \cdot \omega \qquad (1)$$

where, $(k_t, k_v)$ are the torque and back emf constants, $(k_v \cdot \omega)$ is the induced back voltage in the armature.

A general dynamic model parameterized to represent the most common types of rechargeable batteries is implemented by the battery model. The battery is represented as a series resistor with a charge-dependent voltage source, whose voltage is determined by the reciprocal relationship below as a function of charge. The voltage between the battery terminals, V, is determined using the following formula for a given battery nominal voltage, Vo:

$$V = V_o \cdot \left( 1 - \frac{\alpha \cdot (1 - x)}{1 - \beta \cdot (1 - x)} \right) \qquad (2)$$

where $(x)$ is the ratio of the ampere-hours left battery, & $(\alpha, \beta)$ are empirical constants the battery are mentioned in table1.

One important part that directly regulates the power flow between the engine and electric motor is the power split device (PSD). The PSD model takes into account a single-row planetary gear mechanism that is made up of three fundamental parts: a ring gear that mimics the output to the rear axle, a planet carrier with a planetary gear that is linked to the ICE, and a sun gear that is connected to the MG. The planetary gear train may accomplish a range of speed reduction ratios depending on which shaft is stationary, driven, or driving. These ratios depend on their tooth counts as well as the sun and ring radi.

As seen in figure 5 [18], the planetary gear places two kinematic and two geometric restrictions on the three interconnected axes in addition to the fifth constraint, which is the internal wheel (planet).

$$R_C \cdot \omega_C \ = R$$

$$R_R \cdot \omega_R \ = R$$

$$R_C \ =$$

$$R_R \ =$$

The key effective kinematic constraint is given as:

$$(1+\xi_{RS})\cdot\omega_C = \omega_S + \xi_{RS}\cdot\omega_R \tag{7}$$

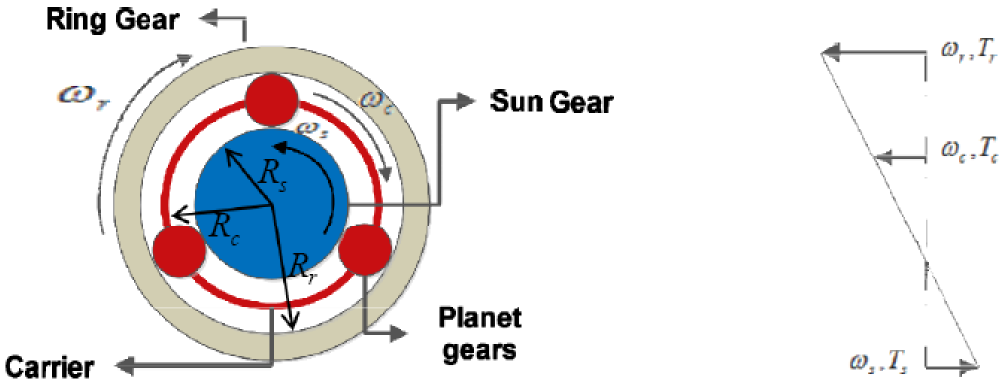


**Fig. 5.** Level diagram analogy of planetary gears.

Two brake band-type actuators regulate the power split device. They all depict frictional brakes, which use a flexible band that encircles the edge of a revolving drum to provide braking force. The band tightens around the revolving drum when a positive actuating force is applied, bringing the friction surfaces into contact. With easily available brake shape and friction characteristics based on the following relationship, the model uses a straightforward parameterization:

$$T_b = F_{in}\cdot\left(e^{\mu\varphi}-1\right)\cdot\tanh\left(\frac{4\omega}{\omega_{th}}\right)\cdot r_d \tag{8}$$

The braking torque $(T)$ is calculated according to required tension force$(F_{in})$ and is restricted by the contact friction coefficient$(\mu)$, wrap angle $(\varphi)$ and the drum radius$(r_d)$. $(\omega,\omega_{th})$ is the shaft angular and threshold speeds, respectively.

According to Table 1, the control system outputs the braking band signals after monitoring the throttle valve position signal and adjusting the motor/generator correspondingly.

The input braking force is fed into the model by a slider gain that controls the brake bands. The motor generator circuit is either grounded or electrified by the motor/generator switch. When parameters are changed, the model reacts instantly, allowing the user to apply and track real-time changes in the dynamics of the model. Together, the controllers form a guide user interface (GUI), which offers an intuitive setting for controlling, observing, and evaluating the system's behavior.

It is assumed that the vehicle body is stiff and that its center of gravity (CG) contains a lumped mass (m). The longitudinal dynamics of the vehicle in the x-direction are described by the single degree of freedom of the vehicle body.

Figure 6-a displays every force influencing the vehicle body, including the forces of gravity (mg), front and rear tire forces (Fxf, Fxr), road inclination (Fd), and aerodynamic drag (Fd). Newton's second law states that the following is the equation of motion in a longitudinal direction:

$$m\cdot\dot{V}_x=\left(F_{xf}+F_{xr}\right)-\frac{1}{2}\rho\cdot C_d\cdot A\cdot\left(V_x-V_D\right)^2-m\cdot g\cdot\sin\beta$$

The generated tire forces are calculated according to Newton's second law as follows

$$I_w\cdot\dot{\Omega}=M_d-F_x\cdot r_d \tag{10}$$

The tire force $(F_x)$ is calculated according to the following tire slip ratio, Figure 6-b

$$slip\ ratio=\frac{\Omega\cdot r_d-V_x}{\Omega\cdot r_d} \tag{11}$$

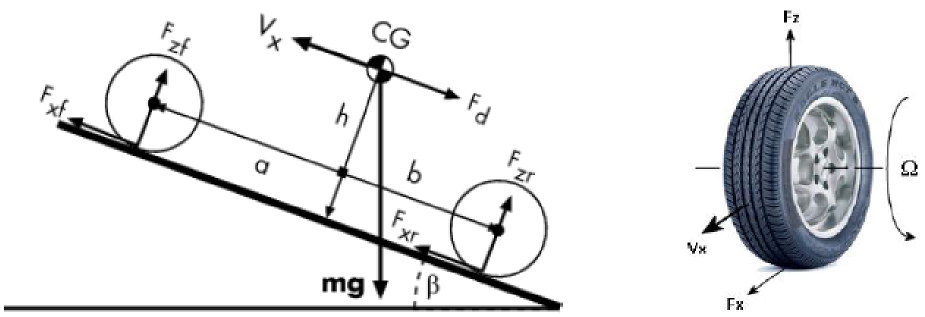


(a) Vehicle Body Forces (b) Tire Forces

**Fig. 6.** Vehicle Body Longitudinal Dynamics.

The model that is being displayed replicates how a HEV would accelerate and decelerate on a level, dry asphalt road.

**Table1:** Modes of operation and control for the proposed model of HEV

| Mode | Brake Band Sun | Brake Band Ring | Description |
|---|---|---|---|
| Charging | OFF | ON | Power is delivered from ICE to the carrier and then to the sun gear. The MG is driven to generate electric energy which is stored in the battery pack. |
| ICE only | ON | OFF | Power is delivered from ICE to the carrier and then to the ring gear. While the MG is off, ICE power drives the vehicle back axle. |
| Synergy | OFF | OFF | Power is delivered from ICE to the carrier and then to the ring gear. While the MG is on, power from both ICE and MG drive the vehicle back axle. |

## RESULTS AND ANALYSIS

### Engine Drive Mode

In this condition, the car is propelled by the engine alone, without the assistance of the MG output power. To stop engine power from flowing to the MG, the MG switch is switched off and the sun side BB2 brake band is applied. 30% is the throttle setting. In Figure 7, the vehicle accelerates to its final speed as the engine accelerates from its idle speed of 800 rpm to 1500 rpm.

### MG Recharging Mode

The engine powers the MG so that it may act as a generator. The MG is driven by the entire engine power when the car is stopped in order to charge the batteries. The sun side BB2's brake band is disengaged, while the ring side BB1's brake band is engaged. As would be expected under comparable engine idle conditions, the throttle valve is set to 5%. In Figure 8, the engine speed increases from 800 rpm, which is the idle speed limit, to 1100 rpm, and the MG speed reaches 3850 rpm. 50% is the starting state of charge for the batteries.

### ICE-MG Synergy Mode

In this mode, the car is empowered by both the MG and ICE outputs. In order to provide electricity to the car simultaneously, the brake bands on the sun and ring sides are both disengaged. In order to compare the power consumption in the two modes, the throttle valve in this mode is set at 30%, just like in Engine Drive Mode. The car accelerates to 111.2 m/s and the engine reaches 1500 rpm in Figure 9. a negative MG rpm value, indicating that its rotating direction is opposite to that of the vehicle's propeller shaft and ICE.
In the engine drive and synergy modes of operation, a fair comparison is made. Table 2 makes it evident that both fuel efficiency and driving mileage are increased while in the synergy mode.

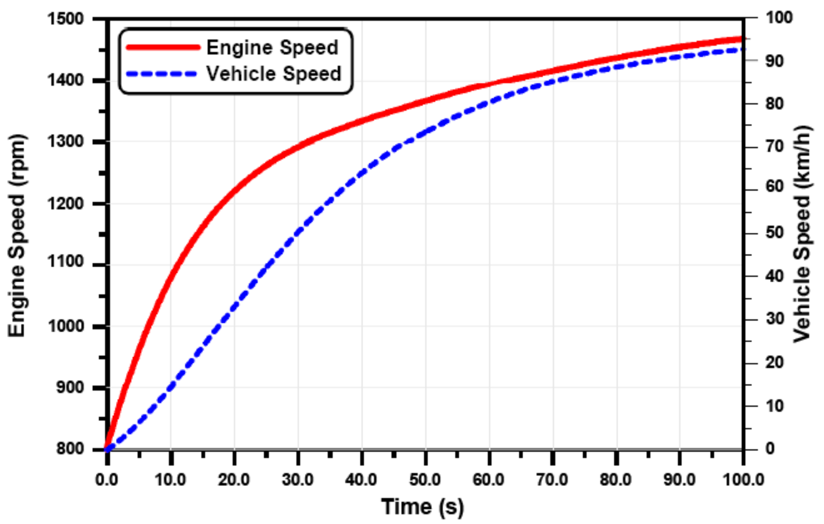


**Fig. 7.** Engine Drive Mode.

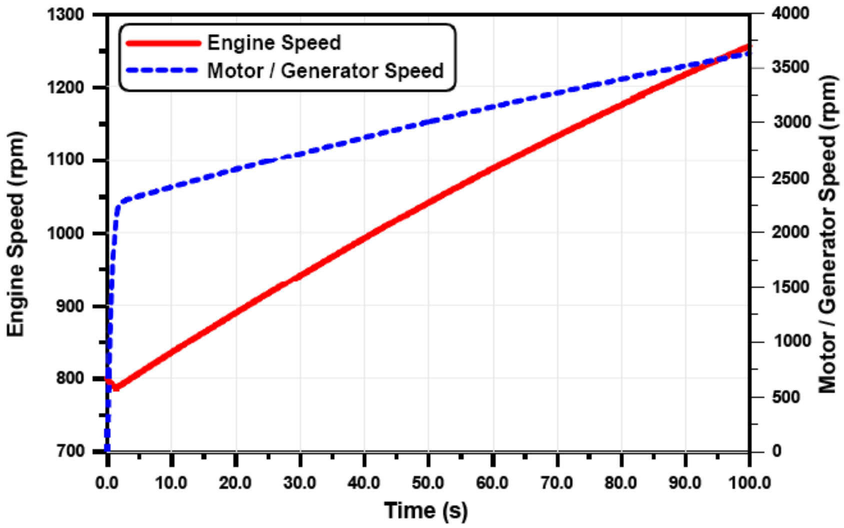


**Fig. 8. Battery Recharging Mode.**

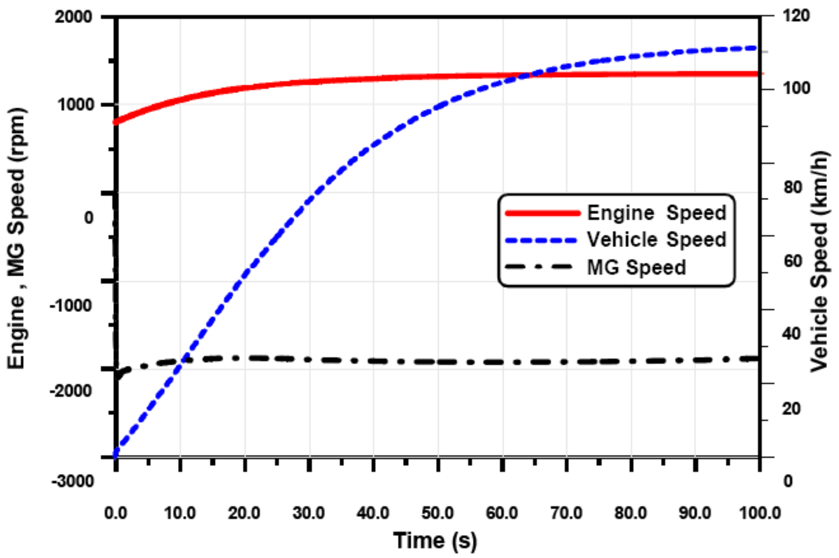


**Fig. 9.** Synergy Mode.

**Table2**: Fuel economy during the engine drive and synergy modes.

| Mode | Engine drive mode | Synergy mode |
|---|---|---|
| Fuel Consumption (G/kW.Hr) | 370.339 | 313.504 |
| Mileage (Km/Liter) | 11.676 | 16.653 |

## CONCLUSIONS

One of the exciting problems in energy management applications is hybrid electric vehicles. Numerous benefits, including reduced emissions and optimized fuel usage, may be obtained by precisely simulating and controlling the various stages of a hybrid power train. This work's suggested model exhibits some encouraging outcomes for the various modes of operation that correspond to the actual situation. Numerous optimization and control techniques may be applied to the model to observe their impact on the overall efficiency of the vehicle since the model operated in an acceptable manner.

## REFERENCES

[1]. The world Factbook, CIA, https://www.cia.gov/library/publications/the-world- factbook/, Last Updated: Apr 19, 2013
[2]. U.S. Energy Information Administration, 'World liquid fuel supply and demand balance', Short-Term Energy Outlook, June– 2013,
[3]. Jinming Liu and Huei Peng, 'Modelling and Control of a Power-Split Hybrid Vehicle, IEEE Transaction of Control Systems

Technology, 2008, Vol.16, No.6
[4]. Cristian Musardo, Giorgio Rizzoni, and Benedetto Staccia, ‘A-ECMS: An Adaptive Algorithm for Hybrid Electric Vehicle Energy Management’, 44th IEEE Conference on Decision and Control, and the European Control Conference, Barcelone, 2005, Spain.
[5]. Manazir Ahmed Khan, ‘Modelling and Simulation of Hybrid Electric Vehicles’, International Journal of Mechanical and Production Engineering, 2013, Vol.1, Issue 3.
[6]. Jinming Liu, Huei Peng and Zoran Filipi, ‘Modeling and Analysis of the Toyota Hybrid System’, International Conference on Advanced Intelligent Mechatronics, 2005, Monterey, California, USA.
[7]. K. Muta, M. Yamazaki, and J. Tokieda, ‘Development of new-generation hybrid system THS II—Drastic improvement of power performance and fuel economy’, SAE, Warrendale, PA, Tech. Rep. 2004-01- 0064, 2004.
[8]. T. Yaegashi, S. Abe, and D. Hermance, ‘Future automotive powertrain—Does hybridization enable ICE vehicles to strive towards sustainable development’, SAE, Warrendale, PA, Tech. Rep. 2004-21-0082, 2004.
[9]. A. Kawahashi, ‘A new-generation hybrid electric vehicle and its implication on power electronics’, The Power Electron Seminar Ind. Rev. (CPES), Blacksburg, VA, Apr. 18–20, 2004.
[10]. Paul Bowles, Huei Peng, Xianjie Zhang, ‘Energy Management in a Parallel Hybrid Electric Vehicle With a Continuously Variable Transmission’, American Control Conference, Chicago, Illinois, USA, 2000.
[11]. Chan-Chiao Lin, Zoran Filipi, Yongsheng Wang, Loucas Louca, Huei Peng, Dennis Assanis and Jeffrey Stein, ‘Integrated, Feed-Forward Hybrid Electric Vehicle Simulation in SIMULINK and its Use for Power Management Studies’, SAE, 2001-01-1334, 2001.
[12]. K.B. Wipke, M.R. Cuddy, and S.D. Burch, ‘ADVISOR 2.1: A User- FriendlyAdvanced Powertrain Simulation Using a Combined Backward/Forward Approach, NREL/JA-540-26839, 1999.
[13]. BMW 850i automatic (1991) full detailed specifications listing and photo gallery, http://www.automobile-catalog.com/auta_details1.php
[14]. J. W. Wong, ‘*Theory of Ground Vehicle*’, 2nd John Wiley, NY 1993.
[15]. Tomas Gillespie, ‘*Fundamentals of Vehicle Dynamics*’, SAE,1992
[16]. Giancarlo Genta, ‘*Motor Vehicle Dynamics: Modelling and Simulation*’, World Scientific Publishing Co. 1997. ISBN 98120229119
[17]. S. Miller and J. Wendlandt. MATLAB News and Notes, 2010
[18]. H. Benford and M. Leising, “The lever analogy: A new tool in transmission analysis,” SAE, Warrendale, PA, Tech. Rep. 810102, 1981.

## **Appendix A:** Vehicle and Simulation Parameters

| **The Vehicle** | | **The Engine** | |
|---|---|---|---|
| Vehicle gross mass (kg) | 1200 | Max. power (kw@rpm) | 175@5000 |
| No. of Driving Axles | 2 | Max. torque (N.m@rpm) | 200@4000 |
| Frontal Area (m²) | 3 | Idle speed (rpm) | 800 |
| Wheel base (m) | 3 | Max. speed (rpm) | 7000 |
| Dynamic radius (m) | 0.3 | | |
| Drag Coefficient | 0.4 | | |
| Rolling res. coefficient | 0.02 | | |
| **Power Split Devise** | | **The Electric System** | |
| Type of planetary GB | Single row | Rated motor speed (rpm) | 2000 |
| Control Actuators | Brake bands | Rated motor power (kw) | 25 |
| Ring to sun ration | 2 | Rated DC voltage (v) | 192 |
| | | Battery voltage (v) | 192 |